Macromolecules

pubs.acs.org/Macromolecules Article

Charge Regulation of Polyelectrolyte Gels: Swelling Transition

Bin Zheng,* Yael Avni, David Andelman,* and Rudolf Podgornik*

Cite This: *Macromolecules* 2023, 56, 5217−5224 Read Online

ACCESS | Metrics & More | Article Recommendations | Supporting Information

ABSTRACT: We study the effects of charge-regulated acid/base equilibrium on the swelling of polyelectrolyte gels by considering a combination of the Poisson−Boltzmann theory and a two-site charge-regulation model based on the Langmuir adsorption isotherm. By exploring the volume change as a function of salt concentration for both nanogels and microgels, we identify conditions where the gel volume exhibits a discontinuous swelling transition. This transition is driven exclusively by the charge-regulation mechanism and is characterized by a closed-loop phase diagram. Our predictions can be tested experimentally for polypeptide gels.

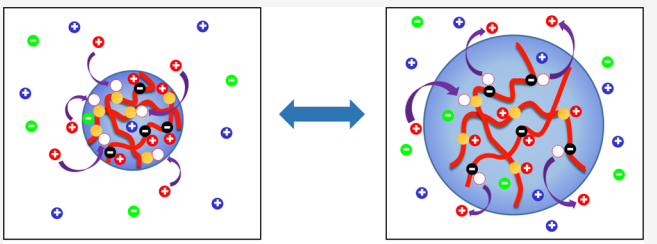

I. INTRODUCTION

Polyelectrolyte (PE) hydrogels[1] are composed of chemically or physically cross-linked PE chains[2] and are ubiquitous in soft biomatter, being a quintessential part of the machinery of life.[3] Apart from applications in controlled encapsulation for drug release, hygiene products, sequestration of ions, and water desalination, they are used as raw materials for biomimetic actuators in soft robotics and therapeutic replacements.[4,5] An important facet of PE hydrogel behavior is the large volume change exhibited by finite-size samples.[6−9] Such an effect is caused by a combination of electrostatic repulsion of charged monomers and osmotic pressure of their counterions.[10,11] Most PE hydrogels contain weakly dissociable acidic or basic groups, which can change their ionization degree upon a change in the solution pH or salt concentration (see ref 1 for a recent review). The gel either releases or withholds protons to/from the bathing solution,[12] and its swelling is sensitive to small variations in these solution parameters.

The swelling of PE hydrogels can be either continuous or discontinuous, as first observed in experiments and later rationalized by Tanaka and co-workers[6,13] using the Donnan equilibrium theory. Those findings indicate that PE hydrogel swelling increases with pH, especially for pH values higher than the pK of ionizable polyacid groups. Furthermore, the swelling can become nonmonotonic for high salt concentrations, first increasing at low salt and then decreasing at higher salt concentrations.

The theoretical analysis of the PE gel swelling was originally centered on the concept of Donnan equilibrium and gel elasticity.[6,13] Later, it was extended[1,14] to include a more detailed description of electrostatic interactions based either on the linear Debye−Hückel theory[15,16] or on the full nonlinear Poisson−Boltzmann (PB) theory, combined with Flory−Huggins theory for polymer mixtures and gel elasticity.[17−21] In addition, there are extensive works done using particle-based models.[22−25]

In previous models, the gel charges were assumed to remain fixed. This constraint was lifted by Muthukumar co-workers,[26,27] who introduced a *self-consistent charge regularization* of the polymer strands. Later on, *charge regulation* (CR) was explicitly introduced into the PE gel theory by Longo *et al.*,[28,29] who described the ability of the PE chains to self-regulate their effective charge through coupling between ionization equilibrium and polymer conformations. A similar line of reasoning was used for PE chains with weakly dissociable groups.[30−32] While the CR modeling in these works is limited to the Langmuir isotherm for a single type of dissociable sites, the general CR phenomenon[33] encompasses also multiple and different types of dissociation sites.[34]

In the present work, we consider both nanogels and microgels, whose size is on the order of 100 nm and 1 μm, respectively,[35,36] and focus on the case of two types of dissociation sites on the PE chains. Specifically, the first type can become negatively charged by deprotonation, while the second can become positively charged by protonation (resulting in a polyampholyte gel).[28,37] We present a mean-field reformulation based on the PB theory coupled to the free energy of a two-site CR model that connects self-consistently the ionic profiles and the PE dissociation state.[33,38,39]

We investigate the effect of salt at neutral pH on the swelling state of a spherical gel sample by demanding the vanishing of

Received: April 4, 2023
Revised: May 28, 2023
Published: June 22, 2023

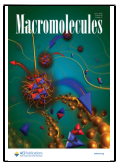

https://doi.org/10.1021/acs.macromol.3c00609
Macromolecules 2023, 56, 5217−5224

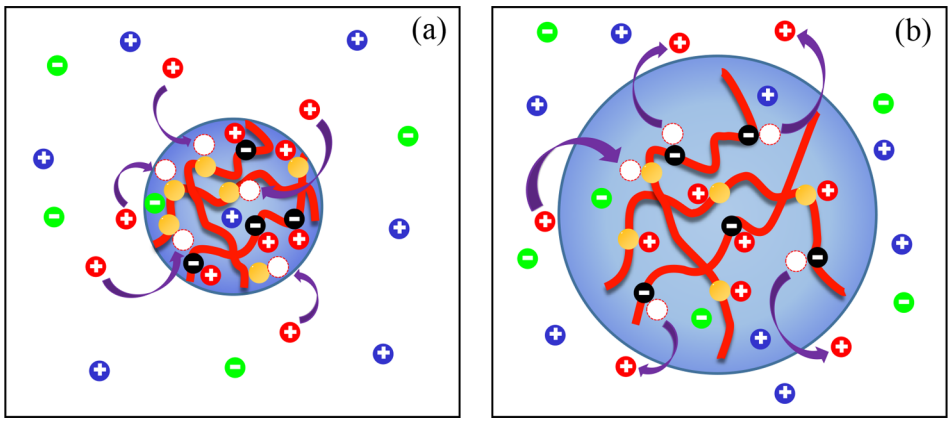

Figure 1. Schematic presentation of two gel states: (a) collapsed state and (b) swollen states for a PE gel with protonation/deprotonation sites, formed by cross-linking N_c polyelectrolyte chains. The gel volume is represented by the blue sphere. In the *two-site model*, the polymer chain has an equal number of *n*-type (deprotonation) and *p*-type (protonation) dissociation sites that can become negatively and positively charged, respectively. The A^- sites and B sites are represented by black and yellow filled circles, respectively. All mobile ionic species, H^+ (red circles), anion (green circles), and cation (blue circles), are exchangeable between the gel volume and bulk bathing solution.

the overall osmotic pressure after the addition of the elastic free energy, just as is done in the standard Flory–Rehner approach.[17] We find an unexpected discontinuous volume transition as a function of the added salt. Moreover, unlike the well-known swelling transition induced by the Flory–Huggins interaction parameter and analyzed *in extenso* in previous works,[15] the new discontinuous volume transition is due exclusively to the CR process itself. It stems directly from the acid–base equilibrium on the polyelectrolyte chains and is somewhat akin to the critical behavior of CR macroions.[40] The corresponding gel charging *via* electrostatic coupling leads to a change in the swelling state, resulting in a phase diagram exhibiting either a continuous or a discontinuous swelling transition with upper and lower critical points.

The outline of the article is as follows. In Section II, we describe the model and the corresponding free energy. Our results are then presented in Section III, where we show the electrostatic potential and polymer charge-density profiles and analyze the gel swelling phase transition as a function of salt concentration and CR parameters. In Section IV, we discuss our findings and make a comparison between the full PB theory and the Donnan approximation. Finally, Section V includes some conclusions relevant to future experiments.

II. MODEL AND FREE ENERGY

We consider a polyampholyte gel composed of N_c cross-linked chains of N monomers each. The gel is immersed in a bathing 1:1 solution containing monovalent ions of bulk concentration $n_+^b = n_-^b = n_b$ and H^+ and OH^- ions with bulk concentrations n_H^b and n_{OH}^b, respectively. The gel chains contain two types of sites: a *p*-site undergoing a protonation and an *n*-site undergoing a deprotonation dissociation reaction. The dissociable group in the *n*-type site is AH and is described by the reaction

$$AH \rightleftarrows A^- + H^+ \tag{1}$$

with the A-site becoming negatively charged in the process, after releasing a proton into the bath. Similarly, the protonation of the *p*-type sites is characterized by an association of a proton from the bath

$$B + H^+ \rightleftarrows BH^+ \tag{2}$$

implying that the B-site becomes positively charged. We assume that there are $N_{site} = \gamma N$ chargeable sites in the gel, characterized by the fraction γ, $0 \le \gamma \le \frac{1}{2}$, and the sites are divided equally into *p*- and *n*-type.

The gel is taken as a sphere of radius R (see Figure 1). Because of the radial symmetry, its properties depend only on the distance from the center, $r < R$. While the concentration of sites is uniform inside the gel, we allow the degree of association/dissociation to vary locally. Hence, we introduce the local charged site fractions, $\phi_p(r)$ and $\phi_n(r)$ for the *p*- and *n*-type sites, respectively, that depend on the radial variable r. $\phi_{n,p}$ varies from zero when the sites at radius r are neutral to 1 when the sites at radius r are fully charged. The fractions $\phi_p(r)$ and $\phi_n(r)$ are considered thermodynamically annealed (adjustable) variables that are coupled to electrostatic potential profile $\psi(r)$. Their thermodynamic equilibrium values are obtained by a variational principle as is explained below.

Equilibrium Thermodynamics. The thermodynamic potential (F) contains several terms that can be written as a volume integral of the electrostatic free energy density (f_{el}), mobile ion translational entropy density (f_{ent}), and the CR free energy density (f_{cr}). Other terms stem from the chemical potentials and the gel elastic free energy (F_{gel})

$$\begin{aligned} F &= \int_V f \, d^3r + F_{gel} \\ &= \int_V d^3r \left(f_{el} + f_{ent} + f_{cr} - \mu_- n_- - \mu_+ n_+ - \mu_H n_H \right. \\ &\quad \left. - \mu_{OH} n_{OH} \right) + F_{gel} \end{aligned} \tag{3}$$

with $\mu_\pm$, μ_H, and μ_{OH} being the chemical potentials of the cations, anions, H^+, and OH^-, respectively. The electrostatic free energy density is given by[41]

$$\begin{aligned} f_{el} &= -\frac{\varepsilon_0 \varepsilon_r}{2} (\nabla \psi)^2 + e\psi \left[n_+ - n_- + n_H - n_{OH} \right. \\ &\quad \left. - (\phi_n - \phi_p) \gamma c_{gel} \mathcal{H}(R - r) \right] \end{aligned} \tag{4}$$

where $n_\pm(r)$, $n_H(r)$, and $n_{OH}(r)$ are the local number densities of cations, anions, H^+, and OH^-, respectively. The last term in the preceding equation corresponds to the net charge density of the polymer chains, where $c_{gel} = N/V_{gel}$ is the average gel

https://doi.org/10.1021/acs.macromol.3c00609
Macromolecules 2023, 56, 5217−5224

concentration, $V_{gel} = 4\pi R^3/3$ is its volume, and $\mathcal{H}(x)$ is the Heaviside step function defined as $\mathcal{H}(x) = 0$ for $x < 0$ and $\mathcal{H}(x) = 1$ for $x \geq 0$.

The translational entropy on the mean-field level comes from all mobile ionic species and can be written in the ideal-gas form[41]

$$f_{ent} = k_B T \sum_{i=\pm,H,OH} n_i[\ln(n_i a^3) - 1] \tag{5}$$

where all ionic species are assumed to have the same molecular volume a^3. The CR term has been discussed extensively in ref 42 and can be written in a general form as

$$f_{cr} = \left[f_n(\phi_n) + f_p(\phi_p)\right]\mathcal{H}(R - r) \tag{6}$$

where a Langmuir adsorption is considered for the charge association/dissociation processes, corresponding to

$$\begin{aligned} f_p(\phi_p) &= (\alpha_p + \mu_p) z_p(\phi_p) + \gamma c_{gel} s(\phi_p) \\ f_n(\phi_n) &= (\alpha_n + \mu_n) z_n(\phi_n) + \gamma c_{gel} s(\phi_n) \end{aligned} \tag{7}$$

where $\alpha_{p,n}$ are the association/dissociation free energy changes for a single p- or n-site, respectively, with charge fractions $z_n(\phi_n) = -\gamma c_{gel}(1 - \phi_n)$ and $z_p(\phi_p) = -\gamma c_{gel}\phi_p$, and $\mu_{p,n} = \mu_H$ in this work, as we assume reactions are protonation/deprotonation processes. Finally, $s(\phi_{p,n})$ is the standard lattice-gas entropy

$$s(x) = k_B T[x \ln x + (1 - x)\ln(1 - x)] \tag{8}$$

The gel elastic energy is computed based on the assumption of an affine deformation[17,43] and depends on the actual model used for the polymer network.[44] For an isotropic deformation, we assume F_{gel} to be of the form

$$F_{gel} = -\frac{3}{2} k_B T N_c \left(\ln \frac{R}{R_0} - \left(\frac{R}{R_0}\right)^2 + 1 \right) \tag{9}$$

where R/R_0 is the swelling ratio, with $R_0 = \eta(N^{1/3}a)$ being a phenomenological *reference radius* parameter, proportional to the radius of the dry gel, in which the polymer sites are assumed to be in their close-packing configuration and η is an adjustable phenomenological parameter that is related to the gel material properties in the experiments. Note that for simplicity we assume that the gel density, distribution of charged groups, and the dielectric constant are homogeneous inside the gel.[45] In addition, the Born energy is not considered as our study is done in the framework of standard Poisson–Boltzmann approximation.[46]

We now define several dimensionless variables, $\tilde{\psi} \equiv e\psi/k_B T$, $\tilde{\mu}_i \equiv \mu_i/k_B T$ for $i = \pm$, H^+, OH^-, and $\tilde{\alpha}_{p,n} \equiv \alpha_{p,n}/k_B T$ to be used hereafter, but for clarity purposes, we drop the tilde from all dimensionless variables.

The thermodynamic equilibrium is then obtained by using a variational principle on the thermodynamic potential F with respect to the annealed variables $n_\pm$, n_H, ψ, and $\phi_{p,n}$. In addition, we assume that the added salt concentration is much larger than H^+, in which case is $n_H^b \ll n_b$. The variation with respect to $n_\pm$ and n_H yields

$$n_\pm(\psi) = n_b e^{\mp\psi}, \quad n_H(\psi) = n_H^b e^{-\psi} \tag{10}$$

where $n_b = n_\pm^b = a^{-3}\exp(\mu_\pm)$ is the bulk salt concentration, taken at zero reference electrostatic potential $\psi = 0$, and $n_H^b = a^{-3}\exp(\mu_H)$.

Variation with respect to ψ yields the mean-field PB equation

$$\begin{aligned} \nabla^2\psi = -4\pi l_B[&n_+(\psi) + n_H(\psi) - n_-(\psi) \\ &- (\phi_n - \phi_p)\gamma c_{gel}\mathcal{H}(R - r)] \end{aligned} \tag{11}$$

where $l_B = e^2/(4\pi\varepsilon_0\varepsilon_r k_B T)$ is the Bjerrum length. For $n_H^b \ll n_b$, the concentration of H^+ in the bulk is negligible as compared to the salt concentration, and the PB equation can be cast as

$$\nabla^2\psi = \kappa^2 \sinh\psi + 4\pi l_B(\phi_n - \phi_p)\gamma c_{gel}\mathcal{H}(R - r) \tag{12}$$

where $\kappa^2 = 8\pi l_B\sqrt{(n_b + n_H^b)n_b} \simeq 8\pi l_B n_b$, and $\kappa = 1/\lambda_D$ is the inverse Debye screening length. For details, see ref 47.

A further variation of the thermodynamic potential with respect to $\phi_{p,n}$ yields the dissociation equilibrium, $\phi_{p,n} = \phi_{p,n}(\psi)$, which looks like a Langmuir isotherm expression

$$\begin{aligned} \phi_n &= \frac{1}{(n_H^b a^3)e^{\alpha_n - \psi} + 1} = \frac{1}{e^{\bar{\alpha}_n - \psi} + 1} \\ \phi_p &= \frac{1}{(n_H^b a^3)^{-1} e^{\psi - \alpha_p} + 1} = \frac{1}{e^{\psi - \bar{\alpha}_p} + 1} \end{aligned} \tag{13}$$

where we defined the following dimensionless parameters $\bar{\alpha}_{p,n} \equiv \alpha_{p,n} + \ln(n_H^b a^3)$.

Finally, after introducing standard forms for the pH and the $pK_{p,n}$, $pH = -\log_{10}(n_H^b a^3)$ and $\alpha_{p,n} = pK_{p,n}\ln 10$, we obtain a simple relation between the pH and the pK's with $\bar{\alpha}_{p,n}$ parameters

$$\bar{\alpha}_{p,n} \equiv -(pH - pK_{p,n})\ln 10 = \alpha_{p,n} - pH \ln 10 \tag{14}$$

where pK_n and pK_p are, respectively, the pK's for the n-type (deprotonation) and p-type (protonation) dissociation sites. Note that the preceding equation is cast in a form analogous to the *charge regulation* boundary condition in the Ninham–Parsegian model,[48] except that the charge regulation is applied here inside the gel volume and not on its surface.

The spatial electrostatic potential and charge profiles, $\psi = \psi(r)$ and $\phi_{p,n} = \phi_{p,n}(r)$, are obtained by solving numerically the PB equation (12) with the finite difference method and the dissociation equilibrium (eq 13) in a spherical geometry, with the boundary conditions $\psi'(0) = 0$ and $\psi'(\infty) = 0$. Note that the electrostatic field at the center of the spherical gel and in the bathing solution has a zero value, dictated by symmetry and electroneutrality in the bulk, respectively.

Finally, the total thermodynamic potential $F_{tot}(R) = \int_V (f - f_b)\, d^3r + F_{gel}$, where f_b = constant is the bulk thermodynamic potential density. The equilibrium gel volume is obtained by minimizing $F_{tot}(R)$ with respect to R, *i.e.*, by setting the osmotic pressure to zero.

III. RESULTS

We consider two different gel sizes: a *nanogel* and a *microgel*. The spherical nanogel has a radius $R = 100$ nm and is made of $N_c = 6$ cross-linked polymer chains. The spherical microgel, on the other hand, has a larger radius in the range of $0.5\ \mu m \leq R \leq 2\ \mu m$ (same parameters as in the expression of ref 17) and is made of $N_c = 6 \times 10^3$ cross-linked chains. For both cases, each

https://doi.org/10.1021/acs.macromol.3c00609
Macromolecules 2023, 56, 5217−5224

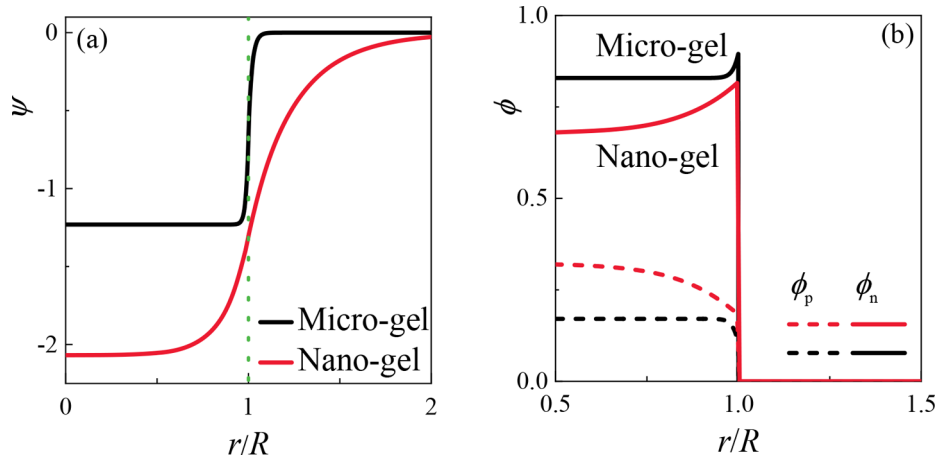

Figure 2. Profiles of (a) electrostatic potential $\psi(r)$ and (b) gel dissociated charge fraction $\phi_{p,n}(r)$ as a function of the dimensionless radial variable r/R for nano- and microgels. The gel radius is R = 30 nm for the nanogel and R = 0.5 μm for the microgel, $\bar{\alpha}_p = \bar{\alpha}_n = -2.3$, and the bulk salt concentration is n_b = 1 mM, corresponding to Debye length of ≃9.6 nm. The dotted green line in (a) represents the location of the gel−solution interface.

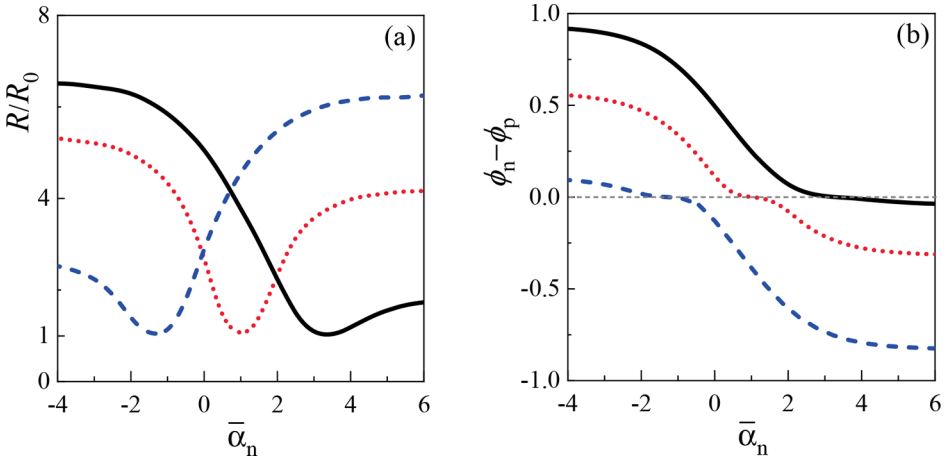

Figure 3. (a) Equilibrium swelling ratio R/R_0 for a nanogel and (b) the corresponding total net charge, proportional to $\phi_n - \phi_p$, as a function of $\bar{\alpha}_n$, for $\bar{\alpha}_p = -2.3$ (black solid line), 0 (red dotted line), and 2.3 (blue dashed line) with n_b = 1 mM. The position of the minimum in the swelling ratio varies as a function of $\bar{\alpha}_p$. The total net charge as a function of $\bar{\alpha}_n$ exhibits a polarity reversal going from positive to negative values through an electroneutral state ($\phi_n = \phi_p$), coinciding with the position of the minimum in the swelling ratio in (a). The microgel case shows similar behavior (not shown here).

polymer chain consists of N = 500 monomers, of which a fraction of γ = 0.5 contains dissociable groups. For simplicity, we assume that the monomers (sites on the chain) and ions have the same size, a = 3.2 Å. At room temperature and in water, the Bjerrum length is l_B = 7.2 Å, bulk pH = 7 is neutral (as in pure water), and the bulk concentration of free ions is in the range 0.01 mM ≤ n_b ≤ 1 mM. Finally, we take η = 5 in defining the phenomenological reference radius parameter for all the numerical examples.

Nanogels and microgels are studied separately in order to explore the differences between the full PB description, based on an explicit solution of the PB equation and a more restrictive *Donnan* description, based on an assumption of a piecewise constant electrostatic potential, being equal to the Donnan potential inside the gel and zero outside. The size difference between nanogels and microgels plays a crucial role in the comparison between the two approaches, which become indistinguishable for large enough ($R \gg \kappa^{-1}$) gel volumes (see Section I of the Supporting Information for details).

The Donnan potential is obtained by assuming a vanishing electrostatic potential outside the gel and enforcing the electroneutrality condition from the PB equation, eq 12, inside the gel with a constant potential ψ_D, which is then obtained as a solution of

$$\kappa^2 \sinh \psi_D + 4\pi l_B \gamma c_{gel}\left(\frac{1}{e^{\bar{\alpha}_n - \psi_D} + 1} - \frac{1}{e^{\psi_D - \bar{\alpha}_p} + 1}\right) = 0 \quad (15)$$

stemming from the full PB equation, eq 12, with the charge regulation conditions, eq 13, included. However, the difference between the nano- and microgel is not restricted only to the quantitative differences between the electrostatic potential and charge density profiles near the gel−solvent interface. As we will show later on, the qualitative behavior of gel swelling is found to be always continuous for nanogels but can be discontinuous for microgels, similar to the case of self-interacting gels with a Flory−Huggins interaction parameter.[13]

https://doi.org/10.1021/acs.macromol.3c00609
Macromolecules 2023, 56, 5217−5224

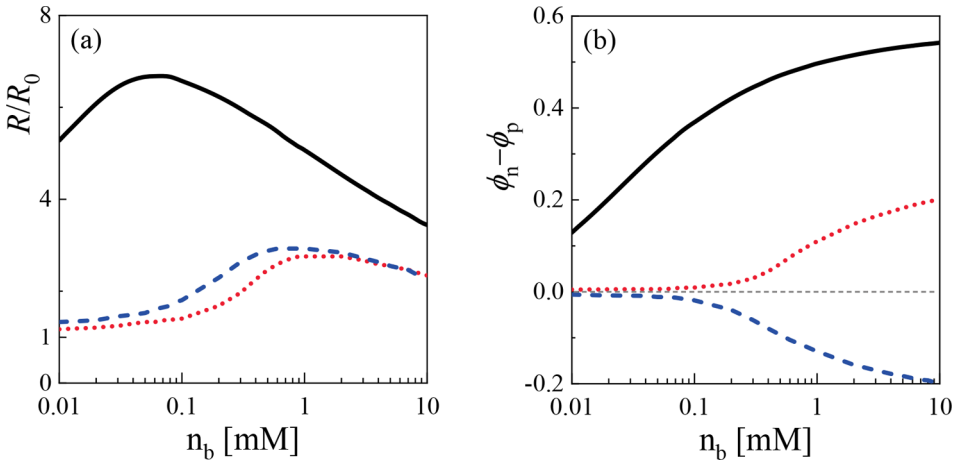

Figure 4. (a) Nanogel equilibrium swelling ratio R/R_0 and (b) its corresponding net charge, proportional to $\phi_n - \phi_p$, as a function of the bulk salt concentration n_b on a semilog plot, for $\bar{\alpha}_p = -2.3$ (solid black line), 0 (red dotted line), and 2.3 (blue dashed line) for fixed $\bar{\alpha}_n = 0$. The thin dashed line in (b) indicates the electroneutral state. The other parameters are $\gamma = 0.5$, $\eta = 5$, and $N = 500$.

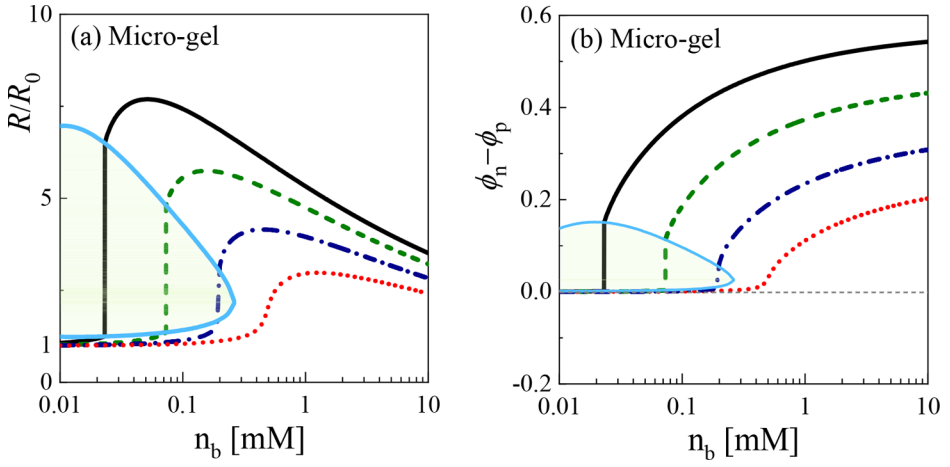

Figure 5. (a) Equilibrium swelling ratio R/R_0 for a microgel and (b) its corresponding net charge, proportional to $\phi_n - \phi_p$, as a function of the salt concentration n_b shown in a semilog plot explicitly for several values of $\bar{\alpha}_p$: $\bar{\alpha}_p = -2.3$ (black solid line), -1.15 (green dashed line), -0.46 (dark blue dash-dotted line), and 0 (red dotted line) for fixed $\bar{\alpha}_n = 0$. A binodal line (light blue) separates in (a) the region that exhibits a discontinuous jump of R/R_0 (light green region) from the region that shows a continuous dependence on n_b. In (b), the region with a discontinuous jump in the net charge is separated from the region that shows a continuous dependence on n_b. The other parameters are $\gamma = 0.5$, $\eta = 5$, and $N = 500$.

Profiles of Electrostatic Potential and Gel Charge Fraction. In Figure 2a we present the electrostatic potential $\psi(r)$ and in Figure 2b the gel dissociated charge fraction, $\phi_{p,n}(r)$, as a function of r, the radial distance from the gel center. The nanogel exhibits a strong variation inside the gel, while for the microgel, the electrostatic potential and dissociated charge fraction are almost constant inside and outside the gel, changing sharply only at the gel−solution interface, having a width comparable to the Debye screening length. This suggests that the Donnan approximation implying a constant electrostatic potential throughout the gel region should work well for microgels but should be qualitatively incorrect for nanogels. The values for Donnan's prediction coincide with the horizontal lines near $r/R = 0$ in Figure 2a. The relationship between the Donnan approximation and the full PB theory is further discussed in Section I of the Supporting Information.

Dependence of the Swelling Ratio and Net Charge on $\bar{\alpha}_n$. The dependence of the swelling ratio R/R_0 on $\bar{\alpha}_n = \alpha_n - \mathrm{pH} \ln 10$, as shown in Figure 3, is nonmonotonic and corresponds to different charging states of the gel. For fixed $\bar{\alpha}_p$, the swelling ratio displays a minimum, observable also in the opposite situation, where we fix $\bar{\alpha}_n$ and vary $\bar{\alpha}_p$.

Depending on the values of $\bar{\alpha}_p$ and $\bar{\alpha}_n$, the gel can become overall positively or negatively charged as is seen in Figure 3. For large negative values of $\bar{\alpha}_n$, the gel is negatively charged with strong swelling. Increasing $\bar{\alpha}_n$ toward positive values causes first a gel contraction until it reaches a minimum size when the overall gel charge vanishes. A further increase in $\bar{\alpha}_n$ then further causes the gel to reverse its polarity and to become positively charged, as is seen in Figure 3b. Note that the magnitudes of the swelling ratio for positive and negative polarity are different. This is a consequence of the charge asymmetry of the system because only H^+ ions are exchanged with the gel, implying that negative and positive polarities are not equivalent. Similar behavior is also observed for the microgel case but is not shown here explicitly.

Discontinuous Swelling of Microgels. Before discussing the interesting case of microgel, we show in Figure 4a the

https://doi.org/10.1021/acs.macromol.3c00609
Macromolecules 2023, 56, 5217−5224

dependence of the swelling ratio R/R_0 on the bulk salt concentration n_b for nanogels. Generally speaking, R/R_0 displays a nonmonotonic dependence on n_b, as the gel size first increases and then decreases. For small n_b values, increasing n_b will increase the dissociation of the AH sites, consequently leading to an interesting observation of *charge-driven swelling* of the gel. As n_b increases even further, the gel charge density gradually reaches a maximal value, while the electrostatic interactions get screened and the osmotic pressure difference between the external bathing solution and the gel decreases, causing a subsequent *charge-driven shrinkage* of the gel.[44] Figure 4b shows that the absolute value of the corresponding net charge of the nanogel is an increasing function of n_b and its polarity depends on the sign of $\bar{\alpha}_p$.

A very different scenario is seen for microgels for combinations of $(\bar{\alpha}_p, \bar{\alpha}_n)$ values as shown in Figures 5a and 5b. Here, the n_b dependence is not continuous everywhere but manifests a discontinuous change (a jump) in the swelling ratio as well as the net charge (see Section II of the Supporting Information for details).

For small values of n_b and when $\bar{\alpha}_n = 0$, the positive and negative charge fractions are approximately equal irrespective of the $\bar{\alpha}_p$ value, resulting in an uncharged gel. As n_b increases, the microgel becomes charged with a polarity that depends on the sign of $\bar{\alpha}_p$. For $\bar{\alpha}_p \leq 0$ shown in Figures 5a and 5b, the negative charge fraction prevails and the polarity of the gel charge is overall negative. Upon increase of n_b, both the charge and the swelling ratio start continuously to increase, as seen in Figure 5a. This increase persists until at some large enough value of n_b the microgel discontinuously charges up and expands by a several-fold increase in the swelling ratio. If n_b is increased even further after the discontinuous jump, the charge of the gel continues to grow, but the swelling ratio first reaches a maximum and then starts decreasing just as in the nanogel case. The existence of the discontinuous jump in the swelling ratio driven solely by charge dissociation and electrostatic interactions is one of our main results and sets the behavior of microgels quite apart from that of nanogels.

The discontinuous jump in the charge and swelling ratio of the gel is not universal but depends on $\bar{\alpha}_p$ and $\bar{\alpha}_n$. For example, having $\bar{\alpha}_n = 0$ and $\bar{\alpha}_p > 0$ leads to continuous swelling and positive polarity (see Section III of the Supporting Information for details). A "binodal line" in the $(R/R_0, n_b)$ "phase diagram" exhibits a critical point (Figure 5a) that separates the region of continuous from discontinuous charging and swelling behavior in the asymmetric charge-regulated PE gels. In fact, the region with discontinuous charging and swelling jumps displays a closed loop in the $(\bar{\alpha}_p, \bar{\alpha}_n)$ plane, as is clear from Figure 6.

Closed-Loop Phase Diagram of Gel Swelling. Referring to the continuous and the discontinuous gel swelling transitions, it would be important to understand the nature of the corresponding phase diagram in the $(\bar{\alpha}_p, \bar{\alpha}_n)$ parameter space, as it gives a better global picture. In Figure 6, we show a *closed-loop* phase diagram where the swelling/charging transition is discontinuous inside the loop, while in the outside region it is continuous. This means that at a fixed $\bar{\alpha}_p$ (or $\bar{\alpha}_n$), while increasing $\bar{\alpha}_n$ (or $\bar{\alpha}_p$), the gel first exhibits a continuous transition and then a discontinuous transition and, finally, it reverts to a continuous transition. Hence, the gel swelling transition is a *re-entrant phase transition*, in terms of system

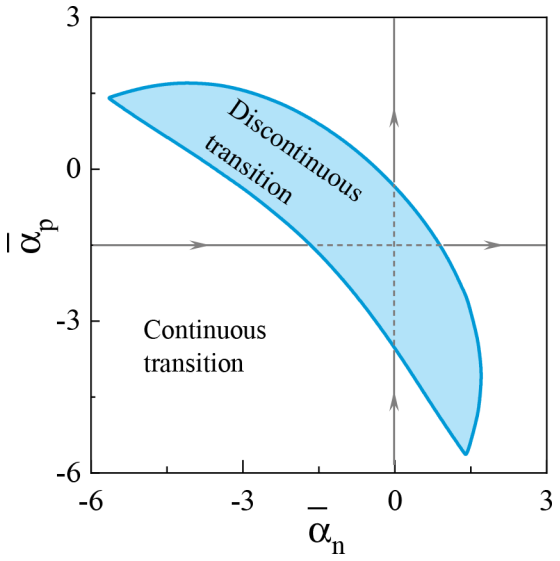

Figure 6. Closed-loop phase diagram of the microgel in the $(\bar{\alpha}_n, \bar{\alpha}_p)$ parameter space. The phase diagram is calculated from the R/R_0 dependence on n_b via the Donnan approximation and exhibits a closed loop, delimiting the discontinuous transition (inner blue region) from the continuous one (outer region). The vertical and horizontal lines are examples of a re-entrant transition through the closed-loop region. On the vertical line $\bar{\alpha}_n$ is being kept constant and $\bar{\alpha}_p$ increases. The role of $\bar{\alpha}_p$ and $\bar{\alpha}_n$ is reserved on the horizontal line.

parameters, $\bar{\alpha}_n$ and $\bar{\alpha}_p$. To connect with the experiment, for polyampholyte proteinaceous gels, one can change $\bar{\alpha}_n$ and $\bar{\alpha}_p$ by varying either the two dissociable amino acid components or the pH.

It is important to stress that these effects are purely mean field in nature and are due to the charge regulation and gel elasticity in charge asymmetric PE gels. They invoke a change in the gel polarity without having to invoke either a Flory–Huggins parameter or steric interactions and correlation effects as is the case in the Voorn–Overbeek type theories.[26,27,30,31,44,49,50]

IV. DISCUSSION

Charge regulation effects in swelling phase transitions and charge separation phenomena of polyelectrolyte (PE) gels and solutions have been considered in the past. Additional related effects such as gel elasticity, the entropy of mixing, counterion adsorption, local dielectric constant, electrostatic interaction among polymer segments, and salt ion correlations have been also explored by analytical theories[26,27] and extensive simulations.[30,44]

However, our main finding is the existence of a continuous/discontinuous swelling phase transition of microgels, driven exclusively by the charge state equilibrium (Figure 5). Such a swelling phase transition is not a consequence of the Flory–Huggins interaction parameter but is connected purely with the changes in the charging equilibrium as described by the CR mechanism. The freedom in the fraction of charged sites, allowed by the CR mechanism, creates two local minima in the free energy: one that has on average neutral sites and a second one with highly charged sites or one that is predominantly positive and the second one that is predominantly negative, depending on the system parameters. The swelling transition occurs when the global minimum changes from one minimum

https://doi.org/10.1021/acs.macromol.3c00609
Macromolecules 2023, 56, 5217–5224

to the other. As is known from statistical mechanics, a true phase transition (with singularities) occurs only in the thermodynamic limit, *i.e.*, when the system size is infinitely large. In our case, we have more pronounced finite-size effects for nanogels where the gel−solution interface plays a more important role than in the larger microgel system. Hence, the phase transition is seen for microgels. We also find that not every charge regulation model results in a reentrant transition, as is seen in the closed-loop phase diagram of Figure 6. The necessary ingredient of the model is the presence of both positively and negatively chargeable subunits as well as a sufficiently large gel size that could be characterized as a microgel.

The nonmonotonic variation of the swelling ratio as a function of the salt concentration in the bathing solution follows from the change in the gel charge. This is a direct consequence of the charge regulation mechanism. The finite size of nanogels smooths the salt dependence of the swelling ratio, while for a large enough volume (microgels), its swelling becomes discontinuous and results in two macroscopic phases.

The relation between charge regulation, as quantified by the two adsorption parameters ($\overline{\alpha}_n$ and $\overline{\alpha}_p$), and electrolyte screening, as quantified by the salt concentration (n_b), then engender a closed-loop phase diagram with an inner region corresponding to a discontinuous swelling. We do not specifically investigate the coupling between the pure CR mechanism and possible nonelectrostatic interactions as quantified by the Flory−Huggins interaction parameter that would result in a more complicated parameter space. The results presented above imply that CR effects pertinent to a PE gel with positively and negatively chargeable subunits can lead to an interesting scenario of swelling phenomena, quite different from what is known for the usual polycationic/polyanionic gels.

V. CONCLUSIONS

In summary, we examined the effect of the charge-regulation mechanism on the swelling behavior of polyelectrolyte gels. We specifically consider a two-site CR model, and the Poisson−Boltzmann theory focuses on elucidating the relationship between the gel volume change and salt concentration for both nanogels and microgels. The findings reveal a discontinuous swelling transition in the gel volume, uniquely driven by the CR mechanism under specific conditions. Moreover, we present a closed-loop phase diagram that identifies these conditions within the parameter space of $\overline{\alpha}_p$ and $\overline{\alpha}_n$.

With the relation between $\overline{\alpha}_p$, $\overline{\alpha}_n$, and the pH and pK of the protonation/deprotonation sites, one can reconstruct the swelling phase diagram using experimental and more accessible variables. This allows a better understanding of possible experimental realizations of our model, for example, a polypeptide gel composed of cross-linked (oligo)peptide chains. Peptide amino acids are one of the most important examples of charge regulation, and their acid/base equilibria have been demonstrated in a variety of other phenomena. We hope that our model will motivate such experimental investigations in the future.

■ ASSOCIATED CONTENT

Supporting Information

The Supporting Information is available free of charge at https://pubs.acs.org/doi/10.1021/acs.macromol.3c00609.

(1) Comparison of PB and Donnan approaches; (2) an analysis of the dependence of thermodynamic potential on swelling ratio for the case of discontinuous gel swelling transition; (3) plot of continuous gel swelling transition; (4) linear plot of Figure 5 (PDF)

■ AUTHOR INFORMATION

Corresponding Authors

Bin Zheng − *Wenzhou Institute, University of Chinese Academy of Sciences, Wenzhou, Zhejiang 325000, China; School of Physics and Astronomy, Tel Aviv University, 69978 Tel Aviv, Israel;* orcid.org/0000-0003-2636-4120; Email: zhengbin@ucas.ac.cn

David Andelman − *School of Physics and Astronomy, Tel Aviv University, 69978 Tel Aviv, Israel;* orcid.org/0000-0003-3185-8475; Email: andelman@post.tau.ac.il

Rudolf Podgornik − *School of Physical Sciences and Kavli Institute for Theoretical Sciences, University of Chinese Academy of Sciences, Beijing 100049, China; Wenzhou Institute, University of Chinese Academy of Sciences, Wenzhou, Zhejiang 325000, China; CAS Key Laboratory of Soft Matter Physics, Institute of Physics, Chinese Academy of Sciences, Beijing 100190, China*; Email: podgornikrudolf@ucas.ac.cn

Author

Yael Avni − *James Franck Institute, University of Chicago, Chicago, Illinois 60637, United States; School of Physics and Astronomy, Tel Aviv University, 69978 Tel Aviv, Israel*

Complete contact information is available at: https://pubs.acs.org/10.1021/acs.macromol.3c00609

Notes

The authors declare no competing financial interest.

■ ACKNOWLEDGMENTS

R.P. acknowledges funding from the Key Project No. 12034019 of the National Natural Science Foundation of China (NSFC) and the hospitality of the School of Physics, University of Chinese Academy of Sciences (UCAS) and Tel Aviv University where this work was completed. D.A. acknowledges the NSFC-ISF Research Program, jointly funded by the NSFC under Grant No. 21961142020 and the Israel Science Foundation (ISF) under Grant No. 3396/19, and ISF Grant No. 213/19. B.Z. acknowledges the NSFC through Grants (No. 22203022) and the Scientific Research Starting Foundation of Wenzhou Institute, UCAS (No. WIUCASQD2022016). Y.A. is thankful for the support of the Clore Scholars Programme of the Clore Israel Foundation and the Zuckerman STEM Leadership Program.

■ REFERENCES

(1) Horkay, F. Polyelectrolyte gels: a unique class of soft materials. *Gels* **2021**, *7*, 102.

(2) Katchalsky, A.; Michaeli, I. Polyelectrolyte gels in salt solutions. *J. Polym. Sci.* **1955**, *15*, 69−86.

(3) Tanaka, T. *From Gels to Life*; University of Tokyo Press: 2004.

(4) *Polymer Gels Perspectives and Applications*; Thakur, V. K., Thakur, M. K., Voicu, S. I., Eds.; Springer: 2018.
(5) Wilcox, K. G.; Kozawa, S. K.; Morozova, S. Fundamentals and mechanics of polyelectrolyte gels: thermodynamics, swelling, scattering, and elasticity. *Chem. Phys. Rev.* **2021**, *2*, 041309.
(6) Tokita, M. Phase transition of gels - a review of Toyoich Tanaka's research. *Gels* **2022**, *8*, 550.
(7) Man, X. K.; Doi, M. swelling dynamics of a disk-shaped gel. *Macromolecules* **2021**, *54*, 4626−4632.
(8) Ding, Z. Y.; Lyu, P. H.; Shi, A.; Man, X. K.; Doi, M. Diffusio-mechanical theory of gel bending induced by liquid penetration. *Macromolecules* **2022**, *55*, 7092.
(9) Osada, Y.; Khokhlov, A. *Polymer Gels and Networks*; CRC Press: 2001.
(10) Jia, D.; Muthukumar, M. Theory of charged gels: swelling, elasticity, and dynamics. *Gels* **2021**, *7*, 49.
(11) Muthukumar, M. 50th anniversary perspective: a perspective on polyelectrolyte solutions. *Macromolecules* **2017**, *50*, 9528−9560.
(12) Hofzumahaus, C.; Strauch, C.; Schneider, S. Monte Carlo simulations of weak polyampholyte microgels: pH-dependence of conformation and ionization. *Soft Matter* **2021**, *17*, 6029−6043.
(13) Ricka, J.; Tanaka, T. Swelling of ionic gels: quantitative performance of the Donnan theory. *Macromolecules* **1984**, *17*, 2916−2921.
(14) Yigit, C.; Welsch, N.; Ballauff, M.; Dzubiella, J. Protein sorption to charged microgels: characterizing binding isotherms and driving forces. *Langmuir* **2012**, *28*, 14373−14385.
(15) English, A. E.; Tanaka, T.; Edelman, E. R. Polyampholytic hydrogel swelling transitions: limitations of the Debye-Hückel Law. *Macromolecules* **1998**, *31*, 1989−1995.
(16) Victorov, A.; Radke, C.; Prausnitz, J. Molecular thermodynamics for swelling of a mesoscopic ionomer gel in 1:1 salt solutions. *Phys. Chem. Chem. Phys.* **2006**, *8*, 264−278.
(17) Colla, T.; Likos, C. N.; Levin, Y. Equilibrium properties of charged microgels: a Poisson-Boltzmann-Flory approach. *J. Chem. Phys.* **2014**, *141*, 234902.
(18) Nikam, R.; Xu, X.; Kanduč, M.; Dzubiella, J. Competitive sorption of monovalent and divalent ions by highly charged globular macromolecules. *J. Chem. Phys.* **2020**, *153*, 044904.
(19) Jha, P. K.; Zwanikken, J. W.; Detcheverry, F. A.; de Pablo, J. J.; Olvera de la Cruz, M. Study of volume phase transitions in polymeric nanogels by theoretically informed coarse-grained simulations. *Soft Matter* **2011**, *7*, 5965−5975.
(20) Claudio, G. C.; Kremer, K.; Holm, C. Comparison of a hydrogel model to the Poisson−Boltzmann cell model. *J. Chem. Phys.* **2009**, *131*, 094903.
(21) Alziyadi, M. O.; Denton, A. R. Osmotic pressure and swelling behavior of ionic microcapsules. *J. Chem. Phys.* **2021**, *155*, 214904.
(22) Mann, B. A.; Holm, C.; Kremer, K. Swelling of polyelectrolyte networks. *J. Chem. Phys.* **2005**, *122*, 154903.
(23) Beyer, D.; Košovan, P.; Holm, C. Simulations Explain the Swelling Behavior of Hydrogels with Alternating Neutral and Weakly Acidic Blocks. *Macromolecules* **2022**, *55*, 10751−10760.
(24) Schneider, S.; Linse, P. Swelling of cross-linked polyelectrolyte gels. *Eur. Phys. J. E* **2002**, *8*, 457−460.
(25) Yin, D.-W.; Yan, Q.; de Pablo, J. J. Molecular dynamics simulation of discontinuous volume phase transitions in highly-charged crosslinked polyelectrolyte networks with explicit counterions in a good solvent. *J. Chem. Phys.* **2005**, *123*, 174909.
(26) Muthukumar, M.; Hua, J.; Kundagrami, A. Charge regularization in phase separating polyelectrolyte solutions. *J. Chem. Phys.* **2010**, *132*, 084901.
(27) Hua, J.; Mitra, M. K.; Muthukumar, M. Theory of volume transition in polyelectrolyte gels with charge regularization. *J. Chem. Phys.* **2012**, *136*, 134901.
(28) Longo, G. S.; Olvera de la Cruz, M.; Szleifer, I. Molecular theory of weak polyelectrolyte thin films. *Soft Matter* **2012**, *8*, 1344−1354.
(29) Longo, G. S.; Olvera de la Cruz, M.; Szleifer, I. Non-monotonic swelling of surface grafted hydrogels induced by pH and/or salt concentration. *J. Chem. Phys.* **2014**, *141*, 124909.
(30) Landsgesell, J.; Sean, D.; Kreissl, P.; Szuttor, K.; Holm, C. Modeling gel swelling equilibrium in the mean-field: from explicit to Poisson-Boltzmann models. *Phys. Rev. Lett.* **2019**, *122*, 208002.
(31) Drozdov, A. D.; Christiansen, D. J. The effects of pH and ionic strength of swelling of cationic gels. *Int. J. Appl. Mech.* **2016**, *8*, 1650059.
(32) Rud, O.; Richter, T.; Borisov, O.; Holm, C.; Košovan, P. A self-consistent mean-field model for polyelectrolyte gels. *Soft Matter* **2017**, *13*, 3264−3274.
(33) Podgornik, R. General theory of charge regulation and surface differential capacitance. *J. Chem. Phys.* **2018**, *149*, 104701.
(34) Borkovec, M.; Jönsson, B.; Koper, G. J. M. Ionization processes and proton binding in polyprotic systems: small molecules, proteins, interfaces, and polyelectrolytes. In *Surface and Colloid Science*; Springer Science, LLC: 2001; pp 99−339.
(35) Ballauff, M.; Lu, Y. Smart" nanoparticles: Preparation, characterization, and applications. *Polymer* **2007**, *48*, 1815−1823.
(36) Karg, M.; Pich, A.; Hellweg, T.; Hoare, T.; Lyon, L. A.; Crassous, J. J.; Suzuki, D.; Gumerov, R. A.; Schneider, S.; Potemkin, I. I.; Richtering, W. Nanogels and microgels: from model colloids to applications, recent developments, and future trends. *Langmuir* **2019**, *35*, 6231−6255.
(37) Longo, G. S.; Olvera de la Cruz, M.; Szleifer, I. Molecular theory of weak polyelectrolyte gels: the role of pH and salt concentration. *Macromolecules* **2011**, *44*, 147−158.
(38) Avni, Y.; Andelman, D.; Podgornik, R. Charge regulation with fixed and mobile charged macromolecules. *Curr. Opin. Electrochem.* **2019**, *13*, 70−77.
(39) Huang, C. H.; Zhu, Y. Y.; Man, X. K. Block copolymer thin films. *Phys. Rep.* **2021**, *932*, 1−3.
(40) Avni, Y.; Podgornik, R.; Andelman, D. Critical behavior of charge-regulated macro-ions. *J. Chem. Phys.* **2020**, *153*, 024901.
(41) Markovich, T.; Andelman, D.; Podgornik, R. Charged membranes: Poisson-Boltzmann theory, DLVO paradigm and beyond. In *Handbook of Lipid Membranes Molecular, Functional, and Materials Aspects*; CRC Press: 2021; pp 99−128.
(42) Avni, Y.; Markovich, T.; Podgornik, R.; Andelman, D. Charge regulating micro-ions in salt solutions: screening properties and electrostatic interactions. *Soft Matter* **2018**, *14*, 6058−6069.
(43) Flory, P. J. Rubber elasticity. In *Principles of Polymer Chemistry*; Cornell University Press: 1953; p 468.
(44) Landsgesell, J.; Beyer, D.; Hebbeker, P.; Košovan, P.; Holm, C. The pH-dependent swelling of weak polyelectrolyte hydrogels is modeled at different levels of resolution. *Macromolecules* **2022**, *55*, 3176−3188.
(45) Ben-Yaakov, D.; Andelman, D.; Harries, D.; Podgornik, R. Beyond standard Poisson-Boltzmann theory: Ion-specific interactions in aqueous solutions. *J. Phys.: Condens. Matter* **2009**, *21*, 424106.
(46) Wang, Z. G. Fluctuation in electrolyte solutions: The self-energy. *Phys. Rev. E* **2010**, *81*, 021501.
(47) By using the identity $-ae^{-x} + be^{x} = 2\sqrt{ab}\,\sinh(x - \ln\sqrt{a/b})$ and rescaling the potential by subtracting the constant $\ln\sqrt{a/b}$ in all formulas, we can derive explicitly the following relation $-4\pi l_B(n_b + n_H^b)e^{-\psi} + 4\pi l_B n_b e^{\psi} = 8\pi l_B[n_b(n_b + n_H^b)]^{1/2}\sinh\psi = \kappa^2\sinh\psi$.
(48) Ninham, B. W.; Parsegian, V. A. Electrostatic potential between surfaces bearing ionizable groups in ionic equilibrium with physiologic saline solution. *J. Theor. Biol.* **1971**, *31*, 405−428.
(49) Salehi, A.; Larson, R. G. A molecular thermodynamic model of complexation in mixtures of oppositely charged polyelectrolytes with an explicit account of charge association/dissociation. *Macromolecules* **2016**, *49*, 9706−9719.
(50) Zheng, B.; Avni, Y.; Andelman, D.; Podgornik, R. Phase separation of polyelectrolytes: The effect of charge regulation. *J. Phys. Chem. B* **2021**, *125*, 7863−7870.

https://doi.org/10.1021/acs.macromol.3c00609
Macromolecules 2023, 56, 5217−5224